PHOBOS'S MINERALOGY REINVESTIGATED. APPLICATION OF THE WAVELET TRANSFORM TO THE ANALYSIS OF ISM/PHOBOS2 INFRARED SPECTRA.

A. Gendrin[1] and S. Erard[2], [1]Institut d'Astrophysique Spatiale, CNRS, Université Paris 11, bâtiment 121, 91405 Orsay Campus, France aline.gendrin@ias.fr, erard@ias.fr.

Introduction: In the study presented here, a technique based on the wavelet transform and described in the accompanying abstract ([1]) is applied to the near-infrared spectra of Phobos obtained by ISM in 1989 from the Phobos-2 spacecraft. Small mineralogical variations are observed across the red, optically altered, unit of Phobos. The mineralogical composition appears to comprise olivine in the whole observed area, while orthopyroxene is detected only in some localised regions.

Method: ISM acquired the only resolved observations of Phobos available in the near infrared. The dataset consists in ~350 spectra with a spatial resolution of ~700m. The 2 detectors of ISM acquired data respectively between ~0.7 and ~1.5 µm with a resolution of ~0.03 µm, and between ~1.6 and ~3.1 µm with a resolution of ~0.06 µm.

Comparisons with UV-Visible data demonstrated that the areas observed by ISM are consistent with optically altered (space-weathered) terrains ([4]). The presence of small mineralogical differences was identified through the dataset ([4]). Here, olivine is observed through the whole observed area, while orthopyroxene is found in only some spatially limited regions. We applied a technique of band detection based on the wavelet transform, and returning the positions, widths, and strengths of all the absorption bands of the spectra in the region examined ([1]). In this study, we used two Paul wavelets with widths of 0.1 and 0.3 µm, for short and long wavelengths respectively (fig 1).
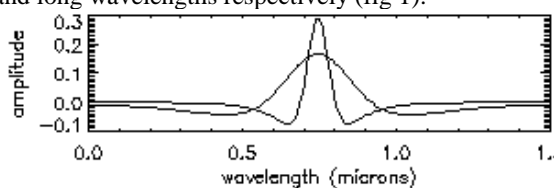

Fig 1: wavelets used in this study

A small difference in viewing directions between the two detectors resulted in a shift between the regions observed at short and long wavelengths. We thus processed each part of the spectrum separately. We first divided the spectra by a continuum linear in energy, i.e. defined by a relationship such as: $y = a/\lambda + b$ where λ is the wavelength ([2]). The parameters a and b were obtained by a linear least square fit of the reflectance, as a function of wavenumbers [2]. This step is performed so as to correct the spectra from the very red slope observed. The fit are good enough to approximate the spectral continuum and characterize the absorption bands with the present method.

An upper estimate of the noise level is derived as follows: we obtained a smoothed spectrum using a Savitzsky Golay filter, and calculated the standard deviation of the difference between the data and the smoothed signal for each channel. We thus obtained the two curves presented in fig 2, one for each detector. In the regions of interest (around 0.85, 1 and 2 µm), the values of the noise level are roughly constant (respectively equal to 0.002, 0.001 and 0.005), and therefore the expected noise on band depths estimates is equal to this value multiplied by the square root of the number of channel used.
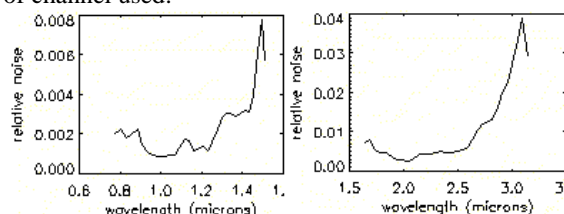

Fig 2: estimated level of noise on the spectra.

Results:

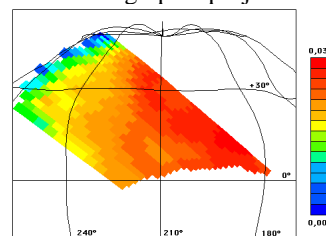Fig 3 shows the location on Phobos of the data presented below. An orthographic projection is used.

Fig 3: Context image of all the images presented below. Reflectance at 0.95 µm.

The wavelet filter detects 2 main bands, at ~1 and ~2 µm, which were already identified ([3],[4]). Here, we find that the 2 µm band is present in only some spatially limited regions. fig. 4 represents its position, obtained as described in [1]. We take into account only the bands with a depth greater than 0.02 which represents 4 times the noise level at this wavelength.
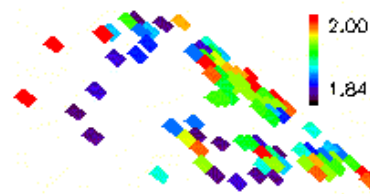

Fig 4: 2 µm band position

PHOBOS'S MINERALOGY REINVESTIGATED: A. Gendrin and S. Erard

In the short wavelengths region, the wavelet filters split the large absorption in 2 components centered at ~0.85 µm and ~1.10 µm, called respectively band 1 and band 2 in the following.

For band 1, we took into account only pixels of depths greater than 0.003, i.e ~1 time the estimated upper limit of noise. Band 1 position exhibits spatial variations correlated with the 2 µm band presence (fig 5). This band is detected at longer wavelengths in the regions where a 2 µm band is present. This fact is not easily observable but can be best seen on the right image of fig 5, on which only the points presenting a wavelength greater than 0.89 µm are shown.
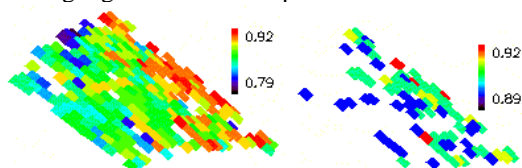

Fig 5:Left: Band 1 position. Right: pixels with band 1 position higher than 0.89 µm.

Band 2 presents wavelength centres at ~1.10 µm. Its depth is ~0.04, ie 3 times above the upper limit of noise level.

All the identified features are interpretable in terms of a mixture of orthopyroxene and olivine. Indeed, the position of the 2 µm feature corresponds to an orthopyroxene band. Band 1 and band 2 are identified as the first 2 components, in order of increasing wavelengths, of the three overlapping bands of olivine in the 1 µm region. Finally, the shift towards longer wavelengths of the ~0.85 µm feature reflects the superposition of the 0.9 µm band of orthopyroxene. The non detection of the third component of the olivine band is attributed to higher values of noise above 1.3 µm and to the choice of a continuum which is not always appropriate in this wavelength region. Moreover, we worked with absolute data, whereas a small uncertainty remains in the calibration of Phobos ISM spectra.

Examples of the 1 µm and 2 µm regions of spectra of the pyroxene-rich region and of the pyroxene-poor region are presented on fig 6 and 7. These spectra are slightly distorted especially because of the continuum chosen, which is not always fully appropriate.

On the spectra of pyroxene-poor areas, a 0.8-1.0 µm band is clearly visible while it disappears in pyroxene-rich regions, which is ascribed to the addition of the 1 µm pyroxene between the two olivine bands (as observed on simulated mixtures). The general shape of the spectra in the pyroxene-poor areas is consistent with olivine.

Attempts were made to obtain the maximum concentration of pyroxene through the method presented in [5], but the absorptions are too shallow and too noisy to obtain this information.
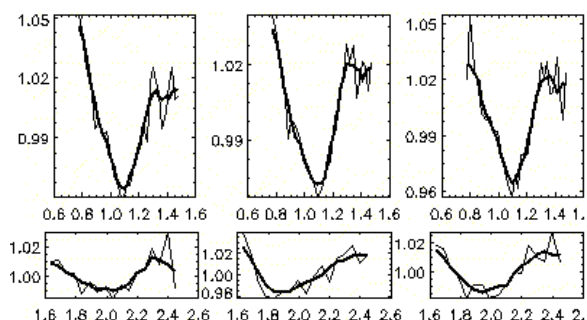

Fig 6:Top: spectra of pyroxene-rich areas at short wavelengths, divided by a continuum as described in text (thick line: smoothed data thin line: original spectra). Bottom: same at long wavelengths.
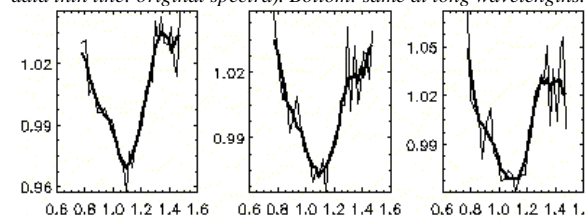

Fig 7: Spectra of the pyroxene-poor area at short wavelengths.

Validation on spectral ratios: A significant problem with the above interpretation is the detection of band 2 at a somewhat too long wavelength, whereas the olivine band is centered at ~1.04 µm. We thus checked our results on spectral ratios. We chose as references spectra presenting no 2 µm band and a 1 µm band as shallow as possible. The results obtained by the band detection algorithm are qualitatively the same. The only significant change is the position of band 2, which is now centered around 1.03 µm (fig 8), in agreement with the olivine band position.

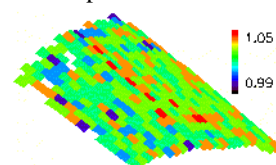*Fig 8: Center of the 1 µm absorption (band 2) obtained from spectral ratios.*

Conclusion: The automatic wavelet-band detection method confirms the widespread occurrence of olivine in the area observed by ISM. A novelty is the variability of both pyroxene absorptions (0.9 and 1.9 µm) in this area. This suggests a variability either in pyroxene abundance, or in space weathering/maturation effects.

Réferences: [1] Gendrin and Erard, this issue. [2] Sunshine J.M. et al. (1990)), *JGR, 95,* 6955-6966. [3] Erard S. (1991), PhD thesis. [4] Murchie S. and Erard S. (1996) *Icarus, 123,* 63-86. [5] Cloutis E.A. et al. (1986), *JGR, 91,* 11,641-11,653.